Journal of Theoretical Biology 498 (2020) 110297

Contents lists available at ScienceDirect

Journal of Theoretical Biology

journal homepage: www.elsevier.com/locate/jtb

Computational analysis of NIRS and BOLD signal from neurovascular coupling with three neuron-system feedforward inhibition network

Anirban Bandyopadhyay, Gaurav Sharma, Shubhajit Roy Chowdhury*

Biomedical Systems Laboratory, Multimedia Analytics, Networks and Systems Group, Indian Institute of Technology Mandi, India

ARTICLE INFO

Article history:
Received 26 January 2020
Revised 29 March 2020
Accepted 26 April 2020
Available online 1 May 2020

Keywords:
Neurovascular coupling unit
Hodgkin-Huxley model
Neurotransmitter
Feedforward-inhibition network
Regional cerebral oxygen saturation

ABSTRACT

Several neurological disorders occur due to hypoxic condition in brain arising from impairment of cerebral functionality, which can be controlled by neural stimulation driven vasoactive response mediated through biological response in astrocyte, a phenomenon known as neurovascular coupling. Brain can adjust with the problem of hypoxic condition by causing vasodilation with the help of this mechanism. To deduce the mechanism behind vasodilation of blood vessel caused by neuronal stimulus, current study articulates a mathematical model involving neuronal system feedforward inhibition network model (FFI) with two other functional components of neurovascular coupling, i.e. astrocyte and smooth muscle cell lining blood vessel. This study includes the neural inhibition network system where glutamatergic pyramidal neuron and GABAergic interneuron act antagonistically with each other. The proposed model successfully includes the implication of the inhibition system to design mathematical model for neurovascular coupling. Result of the proposed model shows that the increase in neuronal stimulus from 20 to 60 $\mu A/cm^2$ has the ability to increase the vasodilatory activity of blood tissue vasculature. Oxygenation level and hemodynamic response due to input synaptic stimulation has been calculated by regional cerebral oxygenation level (rSO_2) and blood oxygen level dependent (BOLD) imaging signal which supports vasodilation of blood vessel with increase in synaptic input stimulus.

1. Introduction

Hypoxic condition in brain results from different deformations in neuronal signal leading to several neurological disorders by Organization (2006). Hypoxic condition in the brain arises due to low oxygenation level in brain due to poor cerebral blood flow (CBF) through blood vessel. So, the proper understanding on in-vivo mechanism of regulating cerebral blood flow is essential to discover possible neurorehabilitation technique to cope up with brain stroke. Brain has its own regulatory mechanisms to combat with hypoxic condition like- neurovascular coupling and cerebral autoregulation. In neurovascular coupling mechanism neuron collaborating with astrocyte function can regulate dilation of blood vessel, which subsequently leads to increase CBF. Cerebral autoregulation process is generally defined by controlling CBF by up and down-regulation of cerebral perfusion pressure (CPP) by Paulson et al. (1990). For greater understanding of mechanism of neurovascular coupling, computational modelling of the biological mechanism of neurovascular coupling associated with neuronal signal and biomechanical response of blood tissue vasculature has been in research domain since the past decade by Cauli and Hamel (2010), Patoary et al. (2019). The relationship between neural activity driven vasoactive response has been recently established through functional magnetic resonance imaging (fMRI) coupled with BOLD imaging signal by Goense et al. (2012), Ray et al. (2015). In several previous studies, aiming to figure out the mechanisms involving neurovascular coupling, mathematical modelling has been designed to elucidate the functional relationship between the components of neurovascular coupling viz. neuronal elements, glial cell astrocyte and smooth muscle lining the blood vessel is commonly known as neurovascular unit (NVU) by Huneau et al. (2015), Keller et al. (2017). A descriptive literature review has been given below in Table 1. to understand the previous work on computational modeling of neurovascular coupling.

In this context of neurovascular coupling, neuronal network analysis is also important. There is an ongoing antagonistic relationship between inhibitory GABAergic neuron and excitatory glutamatergic neuron by Tremblay et al. (2016). The outcome of this conflict is implicated on the glial cell astrocyte for the biological response which affects the vasoactive function of blood vessel. Several experimental and theoretical studies have been done to

* Corresponding author.
E-mail addresses: t18201@students.iitmandi.ac.in (A. Bandyopadhyay), g_sharma@students.iitmandi.ac.in (G. Sharma), src@iitmandi.ac.in (S. Roy Chowdhury).

https://doi.org/10.1016/j.jtbi.2020.110297
0022-5193/

Table 1
Previous mathematical model for neurovascular coupling by Farr and David (2011), Bennett et al. (2008), De Pittà and Brunel (2016), Dormanns et al. (2015), Chander and Chakravarthy (2012), Dormanns et al. (2016), Garnier et al. (2016), Tewari and Majumdar (2012), Witthoft and Karniadakis (2012).

Previous study model	Input	Output	Description
Study1 (Farr and David, 2011)	K^+ and EET	Blood vessel diameter	Study is based on the glutamate and K^+ due to neural activation, which further affects astrocytic Ca^{2+} and EET level leading to impact physio-mechanical events of smooth muscle cell.
Study2 (Bennett et al., 2008)	Glutamate released from glutamatergic synapse	Cerebral blood volume	Study concentrates the theorem that glutamate impacts arteriolar smooth muscle cell diameter through EET level.
Study3 (De Pittà and Brunel, 2016)	Synaptic activity and glutamatergic Glio-transmission	Synaptic plasticity modulation	This core of the study evolves around the idea about Ca^{2+} dependent gliotransmitters released from astrocyte which affects pre-synaptic and post-synaptic plasticity.
Study4 (Dormanns et al., 2015)	Neural activity (K^+ and glutamate in synaptic cleft	Time-dependent radius of blood vessel	A total of 24 coupled ordinary differential equations (ODEs) are designed for neurovascular coupling and are solved using a backward Euler integration with Newton iteration.
Study5 (Chander and Chakravarthy, 2012)	Synaptic current and ATP	Radius of blood vessel	The centre theme of the study is to neural-glial-vessel model based on metabolic and neuronal activity.
Study6 (Dormanns et al., 2016)	Nitric Oxide (NO), glutamate	Radius of blood vessel	Nitric oxide based on neurovascular coupling.
Study7 (Garnier et al., 2016)	Glutamate and GABA neurotransmitter level	Astrocyte activity on neuronal hyperexcitability	Neuron-glia mass model was developed to figure out role of astrocyte in neuronal hyperexcitability.
Study8 (Tewari and Majumdar, 2012)	Glutamate and Ca^{2+}	Astrocytic Ca^{2+} concentration	Tripartite system involving interneuron, pyramidal neuron and astrocyte.
Study9 (Witthoft and Karniadakis, 2012)	Glutamate and K^+	Blood vessel radius	Bidirectional model is developed for neurovascular coupling.

establish the mechanism involving feedforward- inhibition network system (FFI) and the effect of it by Tremblay et al. (2016). The reason behind taking FFI network is that it is the most common and acyclic type. Although none of the earlier studies include this neural network system to study neurovascular coupling response. Previous study model mainly focuses on glutamate released in the synaptic cleft and external K^+ concentration as input signal in the astrocyte by Bennett et al. (2008), Farr and David (2011). Several previous clinical and experimental studies have been done to prove that glutamate/GABA ratio (E/I ratio) is essential to monitor vasodilation and vasoconstriction by Zhou and Yu (2018), Yang and Sun (2018). To fill in the gap between neural network and astrocyte function proposed mathematical model has been developed.

The primary objective of the study is to investigate how different input stimulus impacts neural inhibition network model and vasoactive response from blood vessel. This study also intends to understand how different input stimulus alters cerebral oxygenation level calculated in term of rSO_2 and change in BOLD signal. Though three different pathways have been discovered by which neuronal activation initiate vasodilatory activity, like -through NO (Nitric oxide) mediated diffusion pathway, K^+ channel activated pathway and glutamate induced pathway, this study is focussed on only glutamate activated pathway and how the information has been relayed from a neuronal network to blood vessel through a chain of biological reaction in astrocyte mediated by glutamate neurotransmitters. This paper is organized into following sections- Section 1 deals with introduction and literature review of the topic, Section 2 describes the biological mechanism of neurovascular coupling and how a neurovascular coupling mechanism is impacted by a feedforward-inhibitory type of neuronal network and also deliberates about the mathematical model based on the discussed biological mechanism involving neural network model and Section 3 focuses on the result of the proposed computational model. Section 4 includes the discussion of the work, limitation of the model and the comparative analysis between previous model and the new proposed model and Section 5 includes the concluding remark and future scope of the work.

2. Method and procedure

Mathematical model corresponding to biological mechanism of neurovascular coupling has been discussed in this section. Ongoing biological mechanism in three major components of neurovascular coupling unit viz. neurons, astrocytes and smooth muscle cell lining blood vessel has been deliberated with schematic diagram as shown in Fig. 1.

2.1. Biological mechanism of neurovascular coupling

The mechanism of neurovascular coupling is believed to act through a functional unit called neurovascular unit (NVU)- neuronal network, astrocyte and smooth muscle cell lining blood vessel as shown in Fig. 1.

2.1.1. Feed-forward inhibitory network

Several different neuroinhibitory network has been theoretically and experimentally proven to be present. Among them three are most popularly delineated in earlier literatures by Tremblay et al. (2016), Bacci et al. (2003), Mallet et al. (2005). They

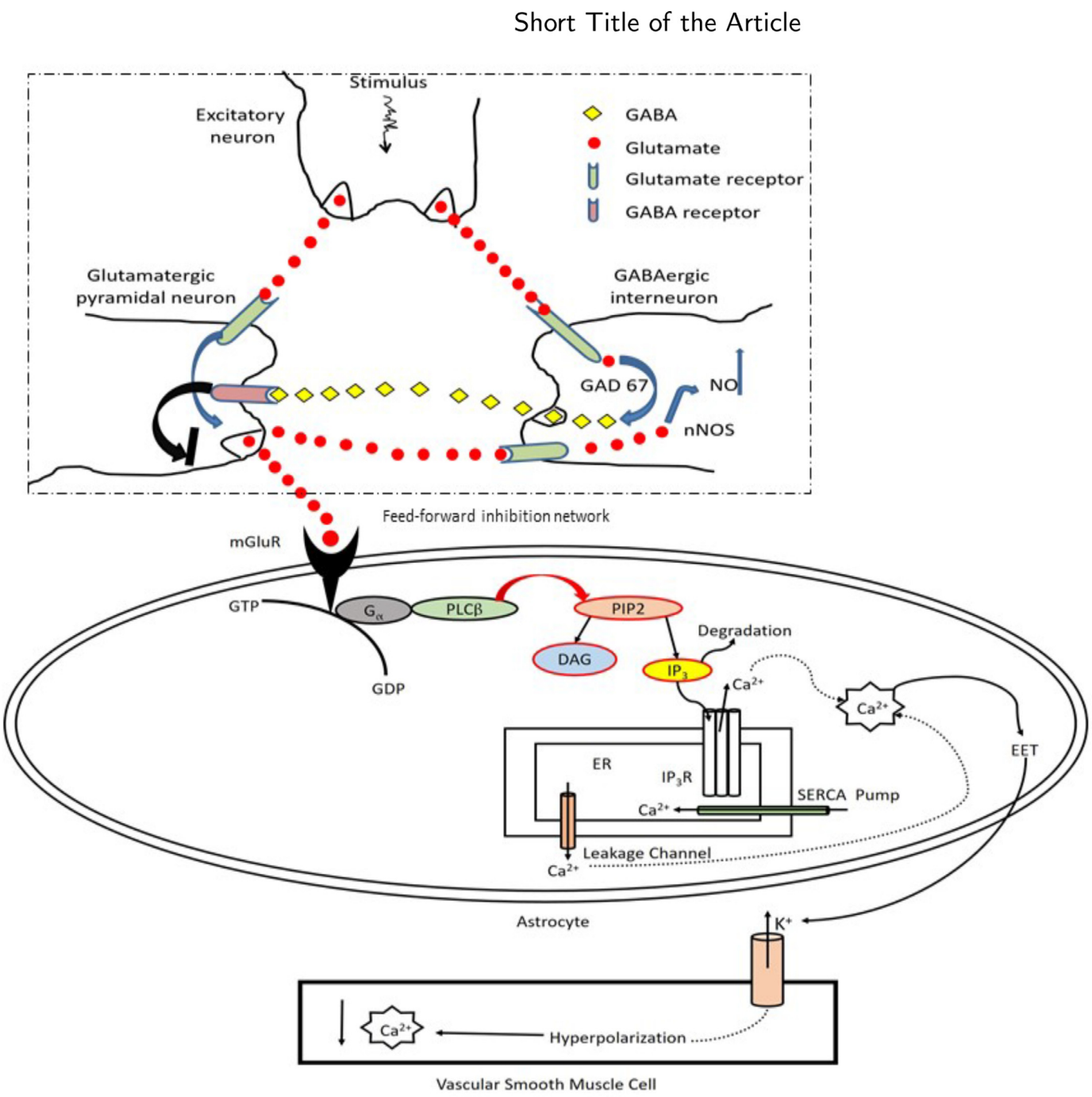

Fig. 1. Biological mechanism of neurovascular coupling with feedforward inhibitory neural network. The biological mechanism of three neuron system has been depicted in the dash-marked in the figure. Glutamate released from the glutamatergic pyramidal neuron after being affcted by the inhibitory GABAergic activity enters into the astrocyte through a G-protein coupled receptor. Activation of the receptor further induces Ca^{2+} production which activates the vascular smooth muscle cell (VSMC) relaxation pathway through a series of biological mechanism.

are- feed-forward inhibitory network (FFI), feedback inhibitory network (FBI) and lateral inhibitory network (LI). These types of network mainly consist of two prominent types of neurons present in the cerebral cortex, excitatory glutamatergic pyramidal neuron and inhibitory GABAergic interneuron. In case of FBI, input synaptic stimulus first excites glutamatergic pyramidal neuron which further excites interneuron. But inhibitory activity of interneuron inhibits pyramidal neuronal activity. Another type of inhibition is called LI, where inhibitory mechanism of interneuron is distinct on the population of pyramidal neuron without being excited by them (Olsen and Wilson, 2008). This paper focuses on the FFI network. Synaptic input stimulus excites excitatory neuron at first which further stimulates inhibitory interneuron and excitatory pyramidal neuron simultaneously by releasing glutamate. Being excited by excitatory neuron, GABA released from interneuron inhibits pyramidal neuron. As shown in Fig. 1, excitatory stimulation through excitatory neuron and inhibitory effect of interneuron both are implicated on pyramidal neuron. Glutamate is converted to GABA by glutamate decarboxylase (GAD 67) in interneuron and incoming glutamate in interneuron leads interneuron to produce NO

(Nitric oxide) by neuronal nitric oxide synthase (nNOS) as depicted in Fig. 1 by Hampe et al. (2017), Tricoire and Tania (2012).

2.1.2. Biological response in astrocyte

Astrocyte is a type of neuroglial cell which supports neuronal function and maintain blood-brain barrier. Glutamate released from glutamatergic pyramidal neuron is taken into astrocyte through metabotropic glutamate receptor (mGluR) by Filosa and Blanco (2007), Bennett et al. (2005). Ligand (glutamate) binds to glutamate receptor resulting activation of G-protein coupled with the receptor. According to the previous studies, IP_3(inositol 1,4,5-trisphosphate) along with diacylglycerol (DAG) is being produced by activity of PLC-β (Phospholipase-C-β) on PIP_2 (Phosphatidylinositol 4,5-bisphosphate) as shown in Fig. 1 by De Pittà et al. (2009). The activity of enzyme is strictly dependent on the surface receptor like- mGluR. The activity of the receptor is dependent on glutamate released from pyramidal neuron and the activity of neuron is strictly dependent on the synaptic stimulus. So, the degradation of IP_3 is regulated by external synaptic stimulus. IP_3 surge causes opening of IP_3 receptor channel IP_3R which consist of one site for IP_3 and other two cites for Ca^{2+} activation and inactivation site. Autocatalytic activity driven by initial Ca^{2+} concentration is prevalent which is driven by initial Ca^{2+} concentration which helps to enhance opening probability of IP_3R which increases intracellular Ca^{2+} concentration. There is a feedback mechanism by which Ca^{2+} influx is possible by Sarco/Endoplasmic Reticulum Ca^{2+} ATPase (SERCA) pump. Thus, there is a Ca^{2+} dynamics influenced by IP_3R is prevalent in astrocyte which influence in Epoxyeicosatrienoic acid (EET) production as depicted in Fig. 1.

2.1.3. Hemodynamic response of neurovascular coupling

With many others, EET is an endothelium derived hyperpolarizing factor (EDHF) which causes relaxation of vascular smooth muscle cell by opening Ca^{2+} activated K^+ channel which causes efflux of K^+ from vascular smooth muscle cell as shown in Fig. 1 by Michaelis and Fleming (2006). Hyperpolarization results relaxation of muscle cell by increasing blood vessel radius and cerebral blood volume. Increase in vasodilation results change in haemodynamic parameters, like- oxy-haemoglobin, deoxy-haemoglobin concentration. Change in vasoactive response initiated by increase of radius of blood vessel causes change in arterial volume and arterial oxygen saturation level associated with it. This change in haemodynamic response can be measured by near infra-red spectroscopy (NIRS). BOLD signal calculates haemoglobin and oxyhaemoglobin level by magnetic relationship of deoxy-haemoglobin which is paramagnetic and oxy-haemoglobin which is di-magnetic. Change in haemodynamic parameters are used to calculate the instantaneous amplitude of BOLD signal. Neuronal activity can also be estimated through BOLD-fMRI signal as more neural activity leads to more vasodilatory activity. With increase of vasodilatory activity haemodynamic response increases.

2.2. Mathematical modelling of neurovascular coupling

A proposed computational and mathematical model for correlating FFI network with astrocyte and smooth muscle cell lining blood vessel has been developed in current study. It is better to understand the functionality of an individual neurovascular coupling unit rather than hundreds of neurons and astrocytes to understand the mechanism of neurovascular coupling. This FFI network system included in this study is composed of three neuronal system, i.e. excitatory neuron, glutamatergic pyramidal neuron and GABAergic interneuron. Output potential of each neuron has been calculated using Hodgkin-Huxley model (HHM) by Hodgkin and Huxley (1952). Neuronal firing from one to another is the input synaptic current. Range of input synaptic current has been taken between 20–60 $\mu A/cm^2$ so that the output membrane potential of each neuron lies between experimentally obtained membrane potential range. This current component is multiplication between output potential of previous neuron and conductivity of the next neuron i.e. (I = EXG). Input stimulus on the pyramidal neuron is the cumulative effect of inhibitory GABAergic interneuron and excitatory neuron. The interlinking parameter between the output of the three neuron-network-system and biological response in astrocyte is activity of metabotropic glutamate receptor ρ(t). Response of biological components in astrocyte has impacted the membrane potential of vascular smooth muscle cell by EET, a vasodilatory molecule. Outcome of neurovascular coupling has been estimated in term of BOLD signal and NIRS signal which indicates oxygenation level. Schematic diagram of mathematical model has been provided in Fig. 2 to elucidate the mathematical model used for articulating computational model for neurovascular coupling with FFI neural network.

2.3. Mathematical model for feedforward inhibitory network system

Input synaptic stimulus with current density ranging between 20 to 60 $\mu A/cm^2$ excites excitatory neuron and the output potential follows Hodgkin-Huxley model. I_{Na}, I_K and I_L indicates Na^+ channel current, k^+ channel current and leakage current.

$$C_m \frac{dV_0}{dt} = I_{Stimulus} - I_{Na} - I_K - I_L \tag{1}$$

Input stimulus of interneuron (I_1) is due to the effect of output potential of excitatory neuron and conductivity (G) of interneuron as shown in Eq. (2). Conductivity of interneuron is the summation of conductivity of sodium channel, potassium channel and leakage current. Output potential of interneuron is simulated by Hodgkin-Huxley model. Parameters used for simulation of Hodgkin-Huxley model has been given in Table 2 below.

$$I_1 = V_0 \times G, \tag{2}$$

$$G = g_{Na} \times m^3 \times h + g_K \times n^4 + g_L \tag{3}$$

$$C_m \frac{dV_1}{dt} = I_1 - I_{Na} - I_K - I_L \tag{4}$$

As discussed earlier, input stimulus current on pyramidal neuron is the outcome of stimulus current coming from excitatory neuron (I_1) and interneuron (I_2). Effect of both stimuluses produce membrane potential (V_2) following Hodgkin-Huxley model.

$$I_2 = V_1 \times G, \tag{5}$$

$$C_m \frac{dV_2}{dt} = (I_1 - I_2) - I_{Na} - I_K - I_L \tag{6}$$

Amount of glutamate released from pyramidal neuron can be calculated using model given in previous studies by Ermentrout and Terman (2010). Parameter value for Eq. (7) is same as taken in the previous study. [$T_{Glutamate}$] indicates glutamate concentration released from pyramidal neuron depending on membrane potential of it.

$$[T_{Glutamate}] \times V_2 = \frac{T_{\max}}{1 + e^{-\left(\frac{V_2 - v_T}{K_p}\right)}} \tag{7}$$

2.4. Mathematical model for biological response in astrocyte

As discussed, earlier glutamate is taken into astrocyte by metabotropic glutamate receptor which is a G-coupled receptor. ρ

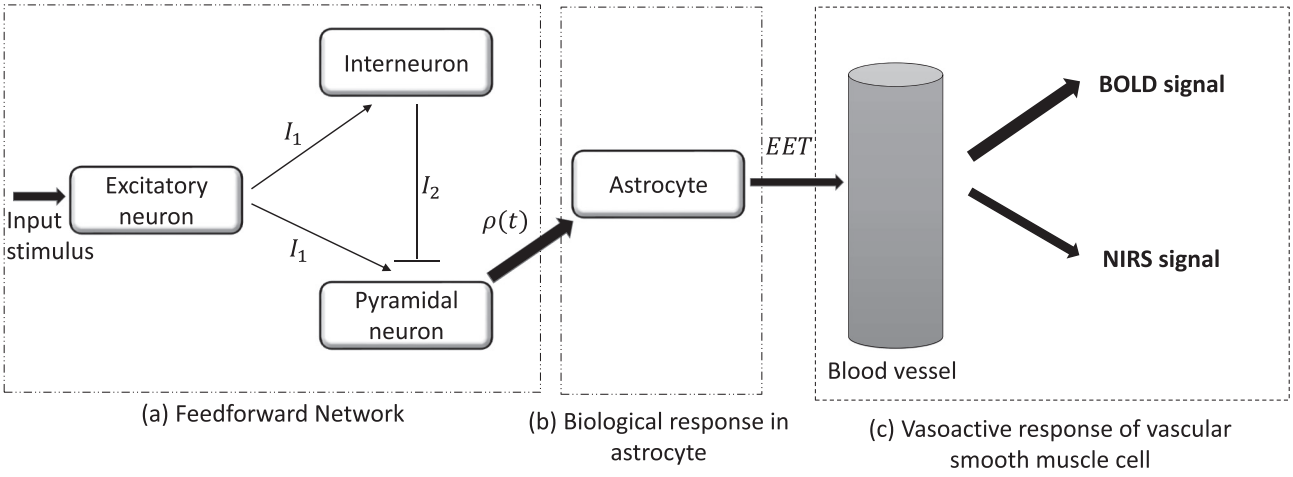

Fig. 2. A schematic digram depicting the mathematical model which is consisted of three major parts segregated by dash-mark. Fig. 2(a) represents three-neuron system feedforward network where output potential due to input stimulus excites interneuron and pyramidal neuron. Inhibitory action of GABAergic interneuron is also taken into account. Fig. 2(b) represents biological function of astrocyte. Fig. 2(c) Outcome of neurovascular coupling which has been calculated in terms of BOLD signal and NIRS signal. ρ(t) is the correlating factor between biological event in neural network and astrocyte. EET (t) is the correlating factor between biological event in biological event in astrocyte and vascular smooth muscle cell.

Table 2
Parameter value for the mathematical model by Hodgkin and Huxley (1952), Bennett et al. (2008), Farr and David (2011), Chander and Chakravarthy (2012), Banaji et al. (2008), Mathias et al. (2018).

Parameters	Description	Value
V_0	Output potential of excitatory neuron in feedforward inhibition	Variable parameter
V_1	Output potential of glutamatergic neuron in feedforward inhibition	Variable parameter
V_2	Output potential of GABAergic neuron in feedforward inhibition	Variable parameter
m	Activation of sodium channels	Variable parameter
h	Inactivation of sodium channels	Variable parameter
n	Activation of potassium channels	Variable parameter
C_m	Equivalence membrane capacitance	1 μF/cm^2
g_{Na}	Sodium channels conductance	120.0 mS/cm^2
g_K	Potassium channels conductance	36.0 mS/cm^2
g_L	Leak channels conductance	0.3 mS/cm^2
E_{Na}	Nernst potentials of sodium ions	115 mV
E_K	Nernst potentials of potassium ions	−12 mV
E_L	Nernst potentials of Leakage ion	10.6 mV
α_m, β_m	Transition rates between open and closed states of the activation of sodium channels	Variable parameter
α_h, β_h	Transition rates between open and closed states of the inactivation of sodium channels	Variable parameter
α_n, β_n	Transition rates between open and closed states of the potassium channels	Variable parameter
I_{Na}	Current due to Sodium channel	Variable parameter
I_K	Current due to potassium channel	Variable parameter
I_L	Current due to leakage current	Variable parameter
T	Concentration of neuro transmitter released from neuron	Variable parameter
$T_{\max}$	Maximum concentration of neurotransmitter	1 mM
K_{deg}	IP_3 degradation rate	1.25 s^{-1}
K_G	G protein dissociation constant	8.82
$r_h{}^*$	Rate of IP_3 production	4.8 μM
$J_{\max}$	Maximum channel current	2880 μMs^{-1}
k_1	IP_3 channel kinetic parameter	0.03 μM
k_{act}	IP_3 channel kinetic parameter	0.17 μM
k_{on}	IP_3 channel kinetic parameter	0.03 μMs^{-1}
k_{inh}	IP_3 channel kinetic parameter	0.01 μM
$[Ca^{2+}]_{ER}$	Ca^{2+} concentration in ER	400 μM
$V_{\max}$	Maximum pumping rate into ER	20 μMs^{-1}
K_p	Dissociation constant of the pump	0.24 uμm
β_{cyt}	Buffer parameter	0.0244
V_{EET}	Rate constant of EET production	72 μM
K_{EET}	Degradation of EET	7.2 μM
γ_{EET}	EET conversion factor	0.004 μMs^{-1}
$r_{\max}$	Maximum radius of the blood vessel at relaxed state	30 μm
$r_{\min}$	Minimum radius of the blood vessel at constricted state	8 μm
$V_{\max}$	Maximum voltage of endothelial muscle cell	−30 mV
$V_{\min}$	Minimum voltage of endothelial muscle cell	−75 mV
SvO_2	Oxygen saturation of venous blood	0.62
SaO_2	Oxygen saturation of arterial blood	0.96
$Hbtot$	Total haemoglobin concentration of arteries and vein	9.1 μM
Vol_n	Normal blood volume as a fraction of brain volume	0.04
τ_{TMT}	Mean transit time	3 s
τ	Parameter corelating CBF and CBV	20 s
d	Empirical relationship between CBF and CBV	0.4

represents amount of bound glutamate in metabotropic glutamate receptor (mGluR). G protein activation and deactivation parameter (G^*) can be calculated by assuming first order kinetics. Previously described model has been followed here to evaluate this parameters by Bennett et al. (2008).

$$\rho = \frac{T_{glutamate}}{K_{glu} + T_{glutamate}} \tag{8}$$

G protein activation and deactivation rate can be determined from following equation.

$$G^* = \frac{\rho + \delta}{K_G + \rho + \delta}; whereas, K_G = \frac{K_d}{K_a} \tag{9}$$

IP_3 concentration in astrocyte can be estimated from production and degradation rate of IP_3 from following equation by Farr and David (2011).

$$\frac{\delta[IP_3]}{\delta t} = r_h \times G^* - K_{deg}[IP3] \tag{10}$$

Ca^{2+} dynamics in astrocyte is dependent on different factors like cytosolic Ca^{2+} concentration change due to functioning of IP3R channel in Endoplasmic reticulum and release of Ca^{2+} on endoplasmic reticulum. $J_{[IP3]}$ represents Ca^{2+} flux from endoplasmic reticulum (ER) to cytosol where J_{pump} represents ATP-dependent flux from cytosol to ER and J_{leak} represents flux from ER to cytosol. β_{cyt} denotes Ca^{2+} buffering in cytosol.

$$\frac{\delta[Ca^{2+}]}{\delta t} = \beta_{cyt}(J_{[IP_3]} - J_{pump} + J_{leak}) \tag{11}$$

$$J_{[IP_3]} = J_{\max}\left[\left(\frac{[IP_3]}{[IP_3] + K_1}\right)\left(\frac{Ca^{2+}}{Ca^{2+} + K_{act}}\right)h\right]^3 \times \left[1 - \frac{Ca^{2+}}{[Ca^{2+}]_{ER}}\right] \tag{12}$$

$J_{\max}$ is the maximum rate of Ca^{2+} flux toward cytosol. K_1 and K_{act} is the dissociation constant forIP_3 and Ca^{2+} binding to IP_3R, h is dynamic variable parameter which denotes the property of IP_3R which is not inactivated by Ca^{2+}. K_{on} and K_{inh} are respectively association and dissociation constant of Ca^{2+} with IP_3R.

$$\frac{dh}{dt} = K_{on}[K_{inh} - (Ca^{2+} - k_{inh})h] \tag{13}$$

$$J_{pump} = V_{\max} \times \frac{[Ca^{2+}]}{[Ca^{2+}] + [K_p]^2} \tag{14}$$

$$J_{leak} = P_L\left(1 - \frac{[Ca^{2+}]}{[Ca^{2+}]_{ER}}\right) \tag{15}$$

$$\beta_{cyt} = \left[\frac{(1 + [B_{end}])}{K_{end}}\right]^{-1} \tag{16}$$

Calcium inducing EET production can be governed by following equation which was also taken in previous study by Farr and David (2011).

$$\frac{d[EET]}{dt} = V_{EET}([Ca^{2+}] - [Ca^{2+}]_{\min}) - K_{EET} \times [EET] \tag{17}$$

2.5. Estimation of vasoactive response of smooth muscle cell lining blood vessel

Hyperpolarization of smooth muscle cell lining blood vessel can be derived from following governing equation by Bennett et al. (2008).

$$\frac{dV_m}{dt} = -\gamma_{EET} \times [EET] \tag{18}$$

A linear correlation has been taken into account between radius of smooth blood vessel and membrane voltage of it by Chander and Chakravarthy (2012).

$$r = r_{\min} + (r_{\max} - r_{\min})\left[\frac{V_{\max} - V_m}{V_{\max} - V_{\min}}\right] \tag{19}$$

Outcome of the neurovascular coupling can be measured by evaluating hemodynamic parameters, like oxy-haemoglobin (HbO_2), deoxy haemoglobin (Hb) and total haemoglobin (Hbt) concentration. Average of the radius of maximum contracted blood vessel and minimum contracted blood vessel has been taken as the baseline radius. Equation governing different haemodynamic parameters has been shown below by Banaji et al. (2008).

$$Hbt = \frac{1000}{4}\left(Vol_{art,n}\left(\frac{r}{r_0}\right)^2 + Vol_{ven}\right) \times Hbtot \times Vol_n \tag{20}$$

$$HbO_2 = \frac{1000}{4}\left(Vol_{art,n}\left(\frac{r}{r_0}\right)^2 SaO_2 + Vol_{ven}SvO_2\right) \times Hbtot \times Vol_n \tag{21}$$

$$Hbt = Hb + HbO_2 \tag{22}$$

Depending on different haemodynamic parameters rSO_2 has been calculated which is recorded through NIRS. rSO_2 can be calculated from hemodynamic parameters like HbO_2 and Hbt.

$$rSO_2 = \frac{HbO_2}{Hbt} \tag{23}$$

Another important parameter which is used to monitor oxygenation level in human brain is BOLD signal. BOLD signal can be evaluated from earlier normalized values of deoxy-haemoglobin and cerebral blood flow using simple mass conservation equation. Compartmental Balloon model has been taken into account for evaluating cerebral blood volume (CBV) by Mathias et al. (2018), Buxton et al. (2004). Equation governing CBV has been given below.

$$\frac{dCBV}{dt} = \frac{1}{\tau_{TMT}}\left(\frac{CBF}{CBF_0} - f_{out}\right) \tag{24}$$

Where, $\frac{CBF}{CBF_0} = \left(\frac{r}{r_0}\right)^4$ and $f_{out} = CBV^{\frac{1}{d}} + \tau\left(\frac{dCBV}{dt}\right)$

Laminar flow has been taken into account for finding relationship between CBF and radius of blood vessel. According to Poiseuille's law, laminar flow in a vessel is proportional to fourth power of the vessel radius. According to the previous study model, change in BOLD signal can be measured from as following.

$$\frac{\Delta S}{S} \approx V_0[a_1(1 - q) - a_2(1 - v)]$$

Where V_0 is the resting venous blood volume fraction (0.03) and a_1 and a_2 are dimensionless physiological parameters ($a_1 = 3.4$, $a_2 = 1.00$) Mathias et al. (2018). q and V represents normalization values for de-oxyhemoglobin and cerebral blood volume.

3. Results

3.1. Neurovascular coupling with feedforward network

Input synaptic stimulus, the driving force of neurovascular coupling, has been provided with current density ranging between 20–60 μA/cm^2 in Hodgkin-Huxley based feedforward inhibition networks. Simulated outcome of the Hodgkin-Huxley based methodology has been depicted in Fig. 3. The membrane potential of excitatory neuron depending on the input stimulus ranging from 20 to 60 μA/cm^2 has been shown in Fig. 3(a). Membrane potential of

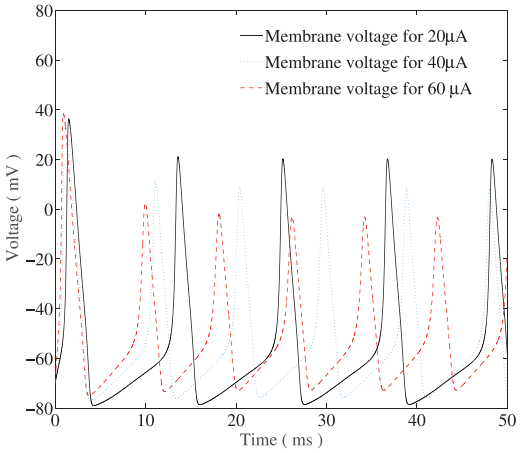

(a) Output potential of excitatory neuron.

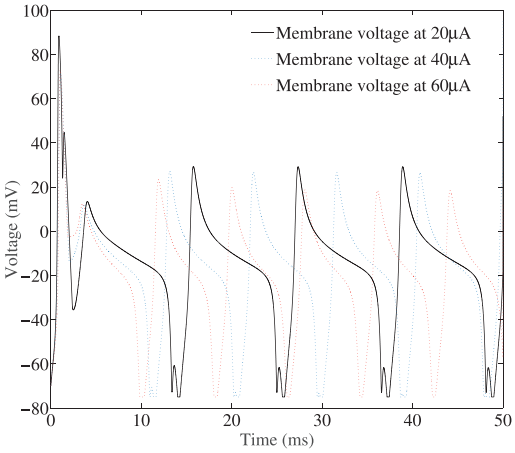

(b) Output potential of GABAergic interneuron.

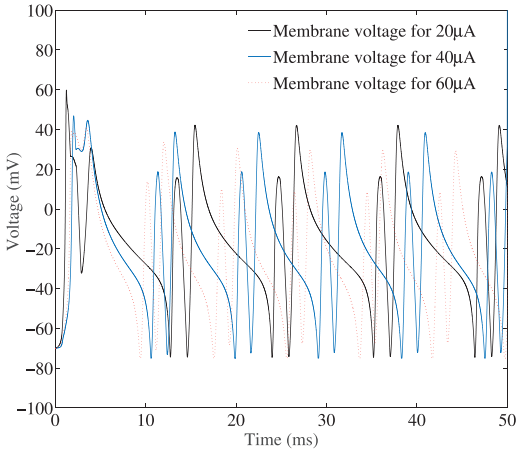

(c) Output potential of glutamatergic pyramidal neuron.

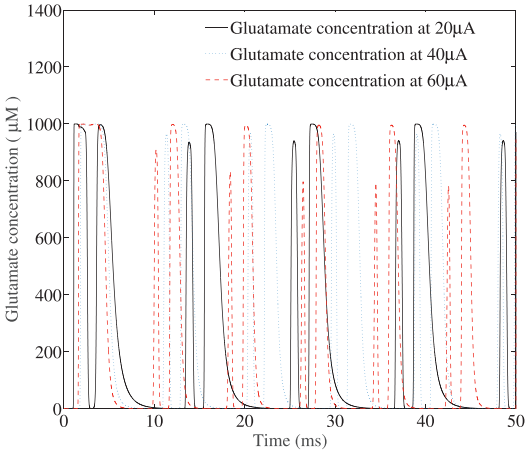

(d) Glutamate concentration released from pyramidal neuron.

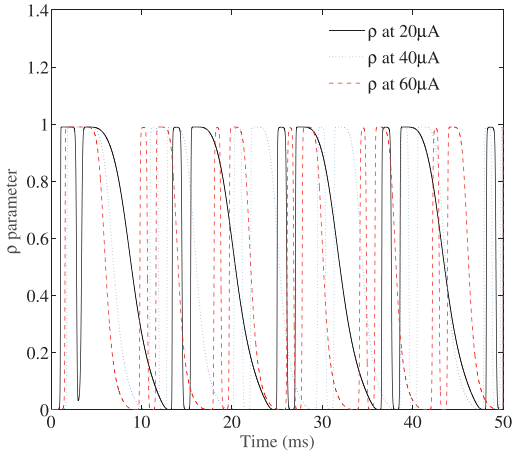

(e) Represents the ρparameter with respect to time.

Fig. 3. Result of Feedforward Inhibition Network for 20, 40 and 60 μA/cm^2. Output potential of excitatory neuron, GABAergic interneuron and pyramidal neuron has been shown in Fig. 3 (a), (b) and (c) respectively. Fig. 3(d) is the simulated outcome of glutamate released from pyramidal neuron and Fig. 3(e) represents the activity of glutamate receptor denoted by ρ(t) parameter. Difference in the outcome of those parameters due to different input synaptic stimulus has been marked differently according to the colour-code given in the top right hand corner of each subfigure.

interneuron arises due to impact of output potential of the excitatory neuron which has been shown in Fig. 3(b). Output potential of interneuron is different from output potential of the excitatory neuron because variable current is input for interneuron. Output potential of pyramidal neuron is the cumulative effect of excitatory signal coming from excitatory neuron and inhibitory signal coming from pyramidal neuron. Every peak gets distorted as shown in Fig. 3(c). because of the inhibitory effect of interneuron. Voltage dependent neurotransmitter released from pyramidal neuron is calculated based on previously described model as given in equation no (7). Alteration of the glutamate concentration signal is based on the change in input synaptic stimulation as shown in Fig. 3(d). Another important aspect of this network model is that with the increase of input stimulus, like from 20 μA/cm^2 to 60 μA/cm^2 number of peaks will be increased. Important observation from Fig. 3(a), (b) and (c) reveals that there is a slight decrease in the amplitude of peaks but number of peaks is increasing with increase of input stimulation because of increase in neuronal activity. ρ parameter represents the binding affinity of the metabotropic glutamate receptor with glutamate neurotransmitter. In earlier studies theoretical value has been taken for this parameter. But in this paper, it has been found that ρ (t) is not a discrete parameter but a continuous function dependent on input stimulus. According to the model described above, ρ(t) has been taken as input signal of astrocyte as shown in Fig. 3(e). As there is more input stimulation, neuronal firing will be increased causing more peak in glutamate concentration which results alteration in ρ(t) parameter.

3.2. Response of biological signal from astrocyte

ρ(t) input signal is used to figure out different biological component concentration i.e. IP_3, Ca^{2+}, EET as discussed in earlier section. Mathematical equations involved in governing IP_3, Ca^{2+} and EET production is given in the section II. The biological signal of these biochemical components producing in astrocyte has been described in the Fig. 4.

Fig. 4 depicts the concentration of biochemical components with respect to feedforward inhibition network. As discussed earlier in biological mechanism, IP_3 production is related to the release of glutamate from pyramidal neuron. IP_3 triggers to pull Ca^{2+} concentration from endoplasmic reticulum of astrocyte which induces Ca^{2+} concentration in the cytosol based on IP_3 concentration in cytosol. Ca^{2+} dynamics in astrocyte plays a major role in vascular activity by initiating the biological mechanism of vasodilation through EET. This model is also able to define alteration in biological signal due to increase of input stimulus. Though there is no significant alteration in peak-amplitude, number of peaks are increased in IP_3, Ca^{2+} and EET concentration as depicted in Fig. 4. From this it is evident that more number of time IP_3, Ca^{2+} and EET achieves maximum concentration and It can be inferred that it is related to increased neuronal firing due to increase of synaptic stimulus from 20 μA/cm^2 to 40 μA/cm^2. Increase in input stimulus causes alteration in ρ(t) signal suggests increase in binding affinity with glutamate receptor. The effect of it is reflected in term of increased number of peaks in biological signal in astrocyte.

3.3. Haemodynamic response of neurovascular coupling

Vasodilatory capacity distinguished in EET enables to hyperpolarize vascular smooth muscle cell resulting in increase in diameter of blood vessel. Haemodynamic parameters (HbO_2, Hb, Hbt) has been calculated in this study taking the average radius as the baseline mentioned above. Vasodilatory action of neurovascular coupling can be estimated through two measuring instruments- NIRS and fMRI. Oxygenation level in brain has been calculated by two parameters rSO_2 and BOLD signal. Vasodilatory activity of blood

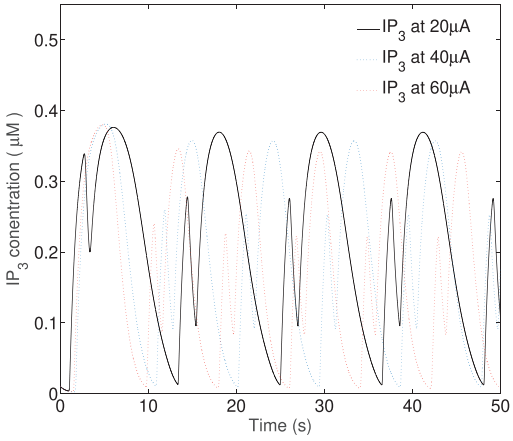

(a) Response of IP_3 concentration.

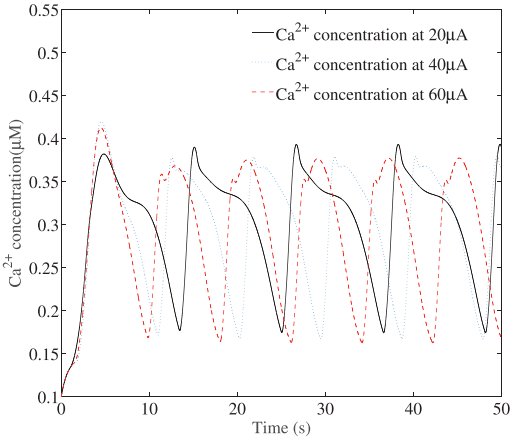

(b) Response of Ca^{2+} concentration.

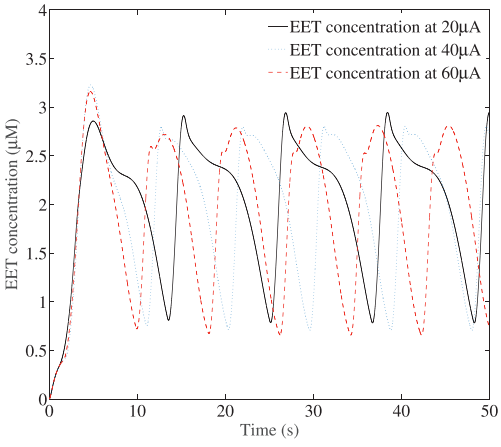

(c) Response of EET production.

Fig. 4. Response of biological signal from astrocyte. Fig. 3 (a), (b), (c) depicts the biological events in the astrocyte due to different input stimulus ranging from 20 μA/cm^2 to 40 μA/cm^2. Alteration of the output i.e. concentration of IP_3, Ca^{2+}, EET due to different input synaptic stimulus has been indicated with different marking code as given in the top most corner of each subfigure.

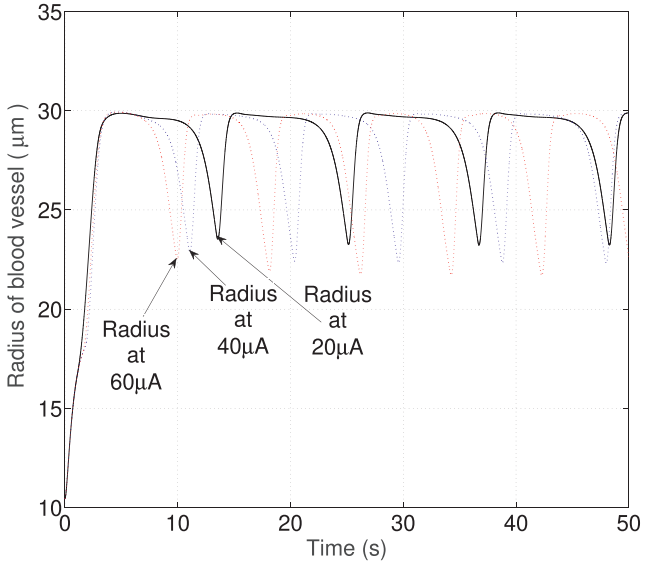

(a) Vasoactive response of vascular smooth blood vessel.

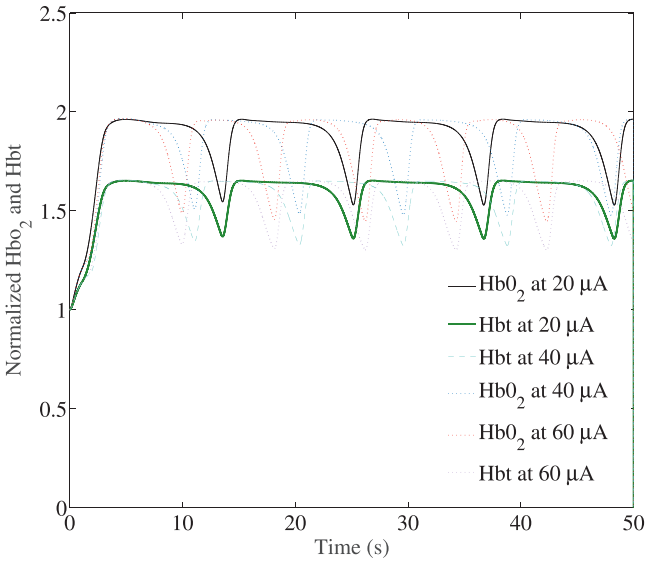

(b) $Hb0_2$, Hb and Hbt based on vasoactive response.

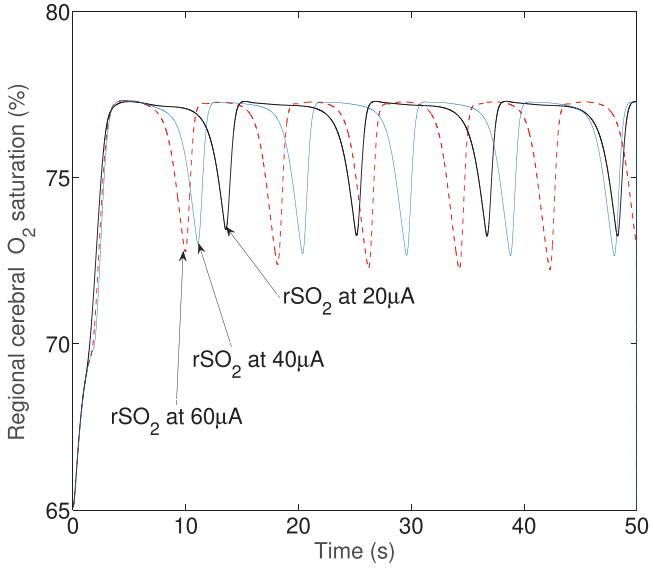

(c) $rS0_2$ based on vasoactive response.

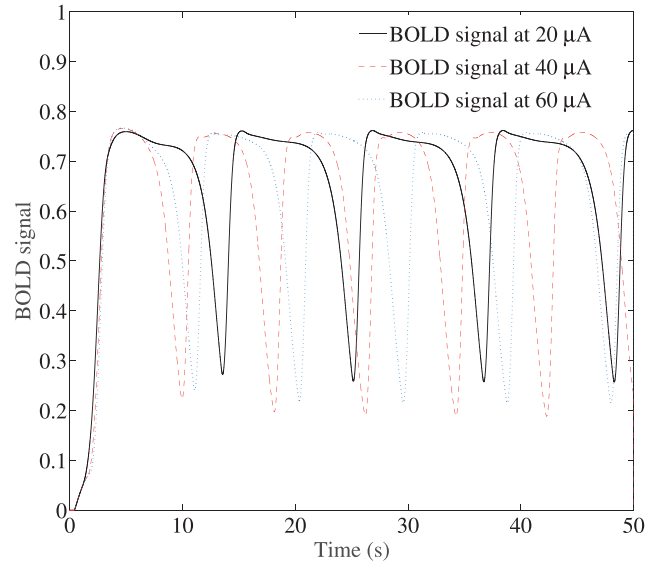

(d) BOLD signal based on vasoactive response.

Fig. 5. Haemodynamic response of neurovascular coupling. Alteration in vascular activity due to different input stimulations have been shown in above figure. Fig. 5(a) gives the idea about frequency of the blood vessel whether Fig. 5(b), (c) and (d) represents the effect in haemodynamic response due to increase in vascular activity. Theoretical estimation of rSo2 and BOLD signal in resoponse to vascular activity has been depicted in Fig. 5 (c) and (d).

vessel can be measured by estimating the radius of smooth blood vessel. As shown in Fig. 5(a) shows response of smooth muscle cell lining blood vessel with respect to different input stimulus. Increase of input stimulus from 20 µA/cm^2 to 40 µA/cm^2 renders increase in number of peaks in signal of radius; four peaks are distinct in case of input current density of 20 µA/cm^2 whether input current density of 40 µA/cm^2 and 60 µA/cm^2 generates five and six peaks respectively. Fig. 5(a) also shows increase in amplitude of peaks in case of 40 µA/cm^2 rather than 20 µA/cm^2 which signifies more vasodilatory capacity with increased input stimulus. With increased current densities of 20, 40 and 60 µA/cm^2 radius of blood vessel increases respectively 6.7, 7.5 and 8.4 µm from its baseline which suggests that increased input stimulus can increase lumen of blood vessel and elevate vasodilatory capacity of smooth muscle cell lining blood vessel. As discussed earlier, oscillation of radius of blood vessel should be between 8 µm to 30 µm (most constriction and most dilation position), though oscillation of lumen of blood vessel is mostly between 21 µm to 30 µm as depicted in Fig. 5(a). There is a significant left shift of the signal of radius of vascular smooth muscle cell which represents more frequent vasoactive response with increase of input stimulus. Peak-analysis of Fig. 5(a) reveals increase in time cycle with decrease in stimulation. i.e. for 20, 40 and 60 uA/cm^2. it is respectively 11.14, 8.93 and 8.13 s.

Impact of the vascular activity is measured in terms of response of hemodynamic parameters, i.e. Oxy-haemoglobin and deoxy-haemoglobin which has been calculated for different input current points as shown in Fig. 5(b). Normalized value of oxy-haemoglobin and deoxy-haemoglobin have been shown at

different current points, i.e. 20–60 uA/cm^2. Calculated regional rSO_2 has been depicted in Fig. 5(c). Saturation level has been found in between 65–75% depending on the HbO_2 and Hb, whether in normal rSO_2 level in human ranges from 60 to 80%. In depth analysis suggests that rSO_2 mostly oscillates between 73–77% which falls in a normal range. With increase of input stimulus, changes in number of peaks have been observed and simultaneously there is increase in peak-amplitude value. As depicted in Fig. 5(c) amplitude of rSO_2 signal has been increased with increase of vasoactive response. Increase in rSO_2 corresponds to the increase of radius of lumen of blood vessel. Another important parameter for evaluating hemodynamic response corresponding to neurovascular coupling is measuring BOLD signal. BOLD signal estimates the oxygenation level in tissue vasculature. Cerebral blood volume as well as de-oxyhaemoglobin, is used to calculated to define BOLD signal. BOLD signal for different input current stimulus has been shown in Fig. 5(d). Normalization value of BOLD signal has been evaluated. There is significant increase in amplitude of BOLD signal as input stimulus increased from 20 μA/cm^2 to 60 μA/cm^2.

4. Discussion

Brain is one of the most active regions which being 2% of total body weight intakes total 20% of cardiac output. Several types of neurons are present in human brain for performing designated function. Two main types of neurons are prevalent in brain- interneuron and pyramidal neuron. Interneuron can be of two types, slow and fast. Pyramidal neuron is also of two types, slow and fast. Interneuron releases GABA which has inhibitory function and glutamate released from pyramidal neuron which is excitatory type. Metabotropic glutamate receptor gets activated by incoming glutamate as well as input stimulation by Keller et al. (2017). Several clinical experimental studies have proved that glutamate and GABA concentration is a regulating factor for the neuronal activity driven neurovascular activity by Lauritzen et al. (2012), Zhou and Yu (2018). This is commonly described by E/I ratio or excitation/inhibition ratio where glutamate is the excitatory type of neurotransmitter and GABA is of inhibitory type. E/I ratio or glutamate/GABA concentration is regulated by neuronal inhibition network system where GABAergic interneuron and glutamatergic pyramidal neuron function antagonistically with each other. This study intends to find out the cumulative effect of antagonistic behaviour on neurovascular coupling mechanism and the impact of increased synaptic stimulus on vasodilatory capacity of smooth muscle cell lining blood vessel. Hodgkin-Huxley model (HHM) has been previously used to study the effect of input synaptic stimulation on trigeminal neuralgia network which have also shown increase of peaks with increase in input synaptic stimulation by Khodashenas et al. (2019). Several theoretical and clinical study has been done to elucidate the underlying mechanism of neurovascular mechanism by Schwartz (2007). fMRI-coupled BOLD signal has been extensively used to study neurovascular coupling. Several neuronal disorders cause malfunction in neurovascular coupling mechanism which can be identified by BOLD signal by estimating the haemodynamic response parameters. Previous studies correlate haemodynamic parameters with oxygenation level defined by BOLD signal to theoretically estimate BOLD signal by Schwartz (2007), Geranmayeh et al. (2015). NIRS is another instrumental technique which is used for estimating oxygenation level by calculating rSO_2. Previous study describes a model based on mathematical study to understand the effect of metabolic and vascular activity in determining cerebral O_2 saturation by Banaji et al. (2008). rSO_2 calculated from the mathematical model described in current study falls in the same range as saturation level from NIRS signal has been obtained from experimentally and mathematically designed model given in earlier study by Banaji et al. (2008). This study not only includes inhibition network to study underlying mechanism of neurovascular coupling but also estimates approximate O_2 saturation by calculating NIRS signal and oxygenation level from BOLD signal.

Result of the proposed model shows increase in number of peaks in vasoactive response from smooth muscle cell lining blood vessel with increase in input current density. The reason behind it lies in increase of neuronal activity of feedforward inhibitory neural network system as well as increase in activity of biological response in astrocyte due to increase in input synaptic stimulus. The elevated vasodilatory activity due to increased number of peaks in radius signal results improvement in cerebral blood flow. So, if there is any need for glucose and O_2 in brain tissue, brain with its self-regulatory mechanism will improve vasodilatory activity of vascular tissue through increasing input synaptic stimulus which has been represented as input current density in current study.

Frequency of vascular activity simulated in the present study as depicted in Fig. 5(d) is congruous with the experimental study done on rat subjects through optical imaging technique by Mayhew et al. (1996). Analysis of this clinical study reveals that the frequency of the vascular activity is around 10 s, which is in the range obtained from the simulation as described earlier (8–11 s). Hemodynamic response function has been later established by accepting this as frequency of vascular activity or 'vasomotion' by Behzadi and Liu (2005). The rSO2 evaluated in the current theoretical study is between 65–75%, which matches with the previously reported clinical studies by Samra et al. (2000), Vretzakis et al. (2014), Tosh and Patteril (2016). BOLD signal obtained from the theoratical study is also comparable with the previous model study by Mathias et al. (2018). However, no experimental study has been done yet to show the hemodynamic response due to different synaptic stimulus i.e. from 20 μA/cm^2 to 60 μA/cm^2; a theoretical study has been done earlier to understand the tripartite system with taking different input stimulus Tang et al. (2013). Although several experimental studies were performed earlier which established the correlation between neural stimulus and cerebral blood flow, BOLD signal by Miller et al. (2001), Frostig et al. (1990). The idea that an increase in input synaptic stimulus can alter the vasodilatory activity of smooth muscle cell lining the blood vessel can be further supported by recent non-invasive brain stimulation based clinical studies by Jindal et al. (2015), Sharma et al. (2019, 2020).

Proposed model depicted in current study is compared against previously explained model which has been shown in below Table 3. The previously described model 1 has taken glutamate released from presynaptic neuron with a theoretical parameter of 2s glutamate signal by Bennett et al. (2008). In model 1, ρ is taken as different discrete value. Maximum peak value of biological signal obtained from this model is dependent on different ρ value. In model 2 provided by Farr and David (2011), Mathias et al. (2018) has taken glutamate and K^+ as input of neurovascular coupling and output of the model gives out vasoactive response, BOLD signal. Oscillation of radius signal remains between 16.5 to 19.5 μm in this computational model. ATP and glutamate as input of neurovascular coupling model has been taken in previously repoted model 3 by Chander and Chakravarthy (2012) where output is vasoactive response and metabolic activity of neurovascular coupling. Oscillation of radius in this model is between 10 to 30 μm which is comparable with the radius signal obtained from the current study. Mathematical model articulated in this study includes neuronal inhibition network and able to depict the increase of vasodilatory activity of smooth muscular cell lining blood vessel with increase in input synaptic stimulus. The current study reveals that increase of input synaptic stimulus has the capability of alteration of radius of blood vessel. Ischemic cerebral stroke is caused by poor cerebral blood flow. This study supports the

Table 3
Comparative analysis of the different mathematical model of neurovascular coupling by Bennett et al. (2008), Farr and David (2011), Chander and Chakravarthy (2012), Mathias et al. (2018).

Models	Neural network network	Input parameter			Biological response in astrocyte			Vasodilatory activity and hemodynamic response		
		Current density	ATP	Glutamate	IP_3	Ca^{2+}	EET	Radius	NIRS signal	Bold signal
Model 1	×	×	×	✓	✓	✓	✓	✓	×	×
Model 2	×	×	×	✓	✓	✓	✓	✓	×	✓
Model 3	×	×	✓	✓	✓	✓	✓	✓	×	×
Proposed model	✓	✓	×	✓	✓	✓	✓	✓	✓	✓

theory of neuronal stimulus driven vasodilatory mechanism of neurovascular coupling and it is useful for understanding underlaying mechanism behind cerebral ischemic stroke by Dutta et al. (2015), Sharma et al. (2019, 2020).

5. Conclusion

Neuronal activity as response of Hodgkin-Huxley based feedforward inhibition network increases with the increase of input synaptic stimulus which also elevates vasodilatory response through a series of biological activities in astrocytes. It can be concluded from the current study that amplified vasodilatory activity in blood vessel with increased input stimulus is due to the improved neuronal activity. Not only that there is significant increase in frequency of vasodilation with increase of input stimulus. Vasodilatory activity and the haemodynamic response because of it can be estimated through fMRI-coupled BOLD signal and NIRS signal. Increase in amplitude of rSO_2 peak and BOLD signal peak also supports the vasodilatory capacity of neuronal stimulus. The ultimate aim of this study is to find out the vasodilatory mechanism due to neurorehabilitation technique which is due to neurovascular coupling. Such a vasodilatory control mechanism strives to provide an alternative neurorehabilitation therapeutic procedure for ischemic stroke patients.

Author Contributions

All authors having equal contribution in this work.

CRediT authorship contribution statement

Anirban Bandyopadhyay: Methodology, Data curation. **Gaurav Sharma:** Visualization, Formal analysis, Writing - original draft. **Shubhajit Roy Chowdhury:** Conceptualization, Writing - review & editing.

Acknowledgment

This work was supported by Indian Institute of Technology Mandi, IITM/DeitY/MLA/ASO/77 India, Ministry of Electronics and Information Technology (MeitY) PhD-MLA/4(22)/2015-2016 and Govt. of India. We would like to thank Mr. Avinash Kumar for his significant suggestions.

References

Bacci, A., Huguenard, J.R., Prince, D.A., 2003. Functional autaptic neurotransmission in fast-spiking interneurons: a novel form of feedback inhibition in the neocortex. J. Neurosci. 23 (3), 859–866.
Banaji, M., Mallet, A., Elwell, C.E., Nicholls, P., Cooper, C.E., 2008. A model of brain circulation and metabolism: NIRS signal changes during physiological challenges. PLoS Comput. Biol. 4 (11), e1000212.
Behzadi, Y., Liu, T.T., 2005. An arteriolar compliance model of the cerebral blood flow response to neural stimulus. Neuroimage 25 (4), 1100–1111.
Bennett, M., Farnell, L., Gibson, W., 2005. A quantitative model of purinergic junctional transmission of calcium waves in astrocyte networks. Biophys. J. 89 (4), 2235–2250.
Bennett, M., Farnell, L., Gibson, W., 2008. Origins of blood volume change due to glutamatergic synaptic activity at astrocytes abutting on arteriolar smooth muscle cells. J. Theor. Biol. 250 (1), 172–185.
Buxton, R.B., Uludağ, K., Dubowitz, D.J., Liu, T.T., 2004. Modeling the hemodynamic response to brain activation. Neuroimage 23, S220–S233.
Cauli, B., Hamel, E., 2010. Revisiting the role of neurons in neurovascular coupling. Front Neuroenerg. 2, 9.
Chander, B.S., Chakravarthy, V.S., 2012. A computational model of neuro-glio-vascular loop interactions. PLoS ONE 7 (11), e48802.
De Pittà, M., Brunel, N., 2016. Modulation of synaptic plasticity by glutamatergic gliotransmission: a modeling study. Neural Plast. 2016.
De Pittà, M., Goldberg, M., Volman, V., Berry, H., Ben-Jacob, E., 2009. Glutamate regulation of calcium and ip 3 oscillating and pulsating dynamics in astrocytes. J. Biol. Phys. 35 (4), 383–411.
Dormanns, K., Brown, R., David, T., 2016. The role of nitric oxide in neurovascular coupling. J. Theor. Biol. 394, 1–17.
Dormanns, K., Brown, R.G., David, T., 2015. Neurovascular coupling: a parallel implementation. Front. Comput. Neurosci. 9, 109.
Dutta, A., Jacob, A., Chowdhury, S.R., Das, A., Nitsche, M.A., 2015. Eeg-nirs based assessment of neurovascular coupling during anodal transcranial direct current stimulation-a stroke case series. J. Med. Syst. 39 (4), 36.
Ermentrout, G.B., Terman, D.H., 2010. Mathematical Foundations of Neuroscience, vol. 35. Springer Science & Business Media.
Farr, H., David, T., 2011. Models of neurovascular coupling via potassium and EET signalling. J. Theor. Biol. 286, 13–23.
Filosa, J.A., Blanco, V.M., 2007. Neurovascular coupling in the mammalian brain. Exp. Physiol. 92 (4), 641–646.
Frostig, R.D., Lieke, E.E., Ts'o, D.Y., Grinvald, A., 1990. Cortical functional architecture and local coupling between neuronal activity and the microcirculation revealed by in vivo high-resolution optical imaging of intrinsic signals.. Proc. Natl. Acad. Sci. 87 (16), 6082–6086.
Garnier, A., Vidal, A., Benali, H., 2016. A theoretical study on the role of astrocytic activity in neuronal hyperexcitability by a novel neuron-glia mass model. J. Math. Neurosci. 6 (1), 10.
Geranmayeh, F., Wise, R.J., Leech, R., Murphy, K., 2015. Measuring vascular reactivity with breath-holds after stroke: a method to aid interpretation of group-level bold signal changes in longitudinal fMRI studies. Hum. Brain Mapp. 36 (5), 1755–1771.
Goense, J., Merkle, H., Logothetis, N.K., 2012. High-resolution fMRI reveals laminar differences in neurovascular coupling between positive and negative bold responses. Neuron 76 (3), 629–639.
Hampe, C.S., Mitoma, H., Manto, M., 2017. Gaba and Glutamate: their Transmitter Role in the Cns and Pancreatic Islets. GABA And Glutamate-New Developments In Neurotransmission Research. IntechOpen.
Hodgkin, A.L., Huxley, A.F., 1952. Currents carried by sodium and potassium ions through the membrane of the giant axon of Loligo. J. Physiol. 116 (4), 449–472.
Huneau, C., Benali, H., Chabriat, H., 2015. Investigating human neurovascular coupling using functional neuroimaging: a critical review of dynamic models. Front. Neurosci. 9, 467.
Jindal, U., Sood, M., Dutta, A., Chowdhury, S.R., 2015. Development of point of care testing device for neurovascular coupling from simultaneous recording of EEG and NIRS during anodal transcranial direct current stimulation. IEEE J. Transl. Eng. Health Med. 3, 1–12.
Keller, A.F., Ambert, N., Legendre, A., Bedez, M., Bouteiller, J.-M., Bischoff, S., Baudry, M., Moussaoui, S., 2017. Impact of synaptic localization and subunit composition of ionotropic glutamate receptors on synaptic function: modeling and simulation studies. IEEE/ACM Trans. Comput. Biol.Bioinform. (TCBB) 14 (4), 892–904.
Khodashenas, M., Baghdadi, G., Towhidkhah, F., 2019. A modified Hodgkin–Huxley model to show the effect of motor cortex stimulation on the trigeminal neuralgia network. J. Math. Neurosci. 9 (1), 4.
Lauritzen, M., Mathiesen, C., Schaefer, K., Thomsen, K.J., 2012. Neuronal inhibition and excitation, and the dichotomic control of brain hemodynamic and oxygen responses. Neuroimage 62 (2), 1040–1050.
Mallet, N., Le Moine, C., Charpier, S., Gonon, F., 2005. Feedforward inhibition of projection neurons by fast-spiking GABA interneurons in the rat striatum in vivo. J. Neurosci. 25 (15), 3857–3869.
Mathias, E.J., Kenny, A., Plank, M.J., David, T., 2018. Integrated models of neurovascular coupling and bold signals: responses for varying neural activations. Neuroimage 174, 69–86.

Mayhew, J.E., Askew, S., Zheng, Y., Porrill, J., Westby, G.M., Redgrave, P., Rector, D.M., Harper, R.M., 1996. Cerebral vasomotion: a 0.1-hz oscillation in reflected light imaging of neural activity. Neuroimage 4 (3), 183–193.
Michaelis, U.R., Fleming, I., 2006. From endothelium-derived hyperpolarizing factor (EDHF) to angiogenesis: epoxyeicosatrienoic acids (EETs) and cell signaling. Pharmacol. Ther. 111 (3), 584–595.
Miller, K.L., Luh, W.-M., Liu, T.T., Martinez, A., Obata, T., Wong, E.C., Frank, L.R., Buxton, R.B., 2001. Nonlinear temporal dynamics of the cerebral blood flow response. Hum. Brain Mapp. 13 (1), 1–12.
Olsen, S.R., Wilson, R.I., 2008. Lateral presynaptic inhibition mediates gain control in an olfactory circuit. Nature 452 (7190), 956.
Organization, W.H., 2006. Neurological Disorders: Public Health Challenges. World Health Organization.
Patoary, M.N.I., Tropper, C., McDougal, R.A., Lin, Z., Lytton, W.W., 2019. Parallel stochastic discrete event simulation of calcium dynamics in neuron. IEEE/ACM Trans. Comput. Biol. Bioinf. 16 (3), 1007–1019.
Paulson, O., Strandgaard, S., Edvinsson, L., 1990. Cerebral autoregulation.. Cerebrovasc. Brain Metab. Rev. 2 (2), 161–192.
Ray, M., Kang, J., Zhang, H., 2015. Identifying activation centers with spatial cox point processes using fMRI data. IEEE/ACM Trans. Comput. Biol. Bioinf. 13 (6), 1130–1141.
Samra, S.K., Dy, E.A., Welch, K., Dorje, P., Zelenock, G.B., Stanley, J.C., 2000. Evaluation of a cerebral oximeter as a monitor of cerebral ischemia during carotid endarterectomy. Anesthesiology 93 (4), 964–970.
Schwartz, T.H., 2007. Neurovascular coupling and epilepsy: hemodynamic markers for localizing and predicting seizure onset. Epilepsy Curr. 7 (4), 91–94.
Sharma, G., Bandopadhyay, A., Chowdhury, S.R., 2020. P111 a preliminary study on vascular activity with ischemic stroke rehabilitation technique. Clin. Neurophys. 131 (4), e73–e75.
Sharma, G., Karwal, O., Chowdhury, S.R., 2019. Non invasive brain stimulation study based on ischemic stroke patients. In: 2019 41st Annual International Conference of the IEEE Engineering in Medicine and Biology Society (EMBC). IEEE, pp. 1461–1464.
Tang, J., Luo, J.-M., Ma, J., 2013. Information transmission in a neuron-astrocyte coupled model. PLoS ONE 8 (11), e80324.
Tewari, S.G., Majumdar, K.K., 2012. A mathematical model of the tripartite synapse: astrocyte-induced synaptic plasticity. J. Biol. Phys. 38 (3), 465–496.
Tosh, W., Patteril, M., 2016. Cerebral oximetry. BJA Educ. 16 (12), 417–421.
Tremblay, R., Lee, S., Rudy, B., 2016. GABAergic interneurons in the neocortex: from cellular properties to circuits. Neuron 91 (2), 260–292.
Tricoire, L., Tania, V., 2012. Neuronal nitric oxide synthase expressing neurons: a journey from birth to neuronal circuits. Front. Neural Circuits 6, 82.
Vretzakis, G., Georgopoulou, S., Stamoulis, K., Stamatiou, G., Tsakiridis, K., Zarogoulidis, P., Katsikogianis, N., Kougioumtzi, I., Machairiotis, N., Tsiouda, T., et al., 2014. Cerebral oximetry in cardiac anesthesia. J. Thorac. Dis. 6 (Suppl 1), S60.
Witthoft, A., Karniadakis, G.E., 2012. A bidirectional model for communication in the neurovascular unit. J. Theor. Biol. 311, 80–93.
Yang, W., Sun, Q.-Q., 2018. Circuit-specific and neuronal subcellular-wide EI balance in cortical pyramidal cells. Sci. Rep. 8 (1), 3971.
Zhou, S., Yu, Y., 2018. Synaptic EI balance underlies efficient neural coding. Front. Neurosci. 12, 46.